



Contents lists available at ScienceDirect

Journal of Advanced Research

journal homepage: www.elsevier.com/locate/jare

Dietary n-3 polyunsaturated fatty acids intervention ameliorates cognitive dysfunction in db/db mice by mitigating cortical insulin resistance, mitochondrial dysfunction, and energy metabolism impairment

Yu Liu^{a,1}, Xiaojun Ma^{a,1}, Jingjing Xu^a, Xixiang Wang^a, Lu Liu^a, Xiuwen Ren^a, Chi Zhang^d, Shaobo Zhou^e, Ying Wang^f, Xinjing Guo^{a,b,c,*}, Linhong Yuan^{a,b,c,*}

^a School of Public Health, Capital Medical University, You Anmen Street, Beijing 100069, China

^b Beijing Key Laboratory of Environment and Aging, You Anmen Street, Beijing 100069, China

^c China-British Joint Laboratory of Nutrition Prevention and Control of Chronic Diseases, You Anmen Street, Beijing 100069, China

^d School of Biological Sciences, University of Nebraska-Lincoln, Lincoln, NE Lincoln 1104 T St Manter Hall 402, 68588-0118, USA

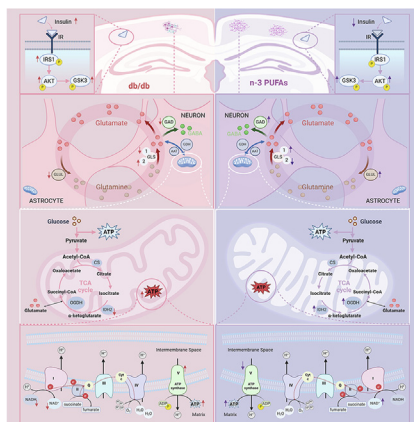
^e School of Science, Faculty of Engineering and Science, University of Greenwich, Central Avenue, Chatham ME4 4TB, United Kingdom

^f Suzhou Research Center of Medical School, Suzhou Hospital, Affiliated Hospital of Medical School, Nanjing University, Lijiang Road, Suzhou 215153, China

HIGHLIGHTS

- db/db mice show distinct insulin resistance and brain mitochondrial dysfunction.
- Abnormal energy metabolism and neurotransmitter cycle underlies cognitive impairment.
- N-3 PUFA intervention effectively alleviates insulin resistance in db/db mice.
- N-3 PUFA reduces neuronal loss and mitochondrial abnormalities in db/db mice.
- N-3 PUFA improves energy metabolism and cognitive function in db/db mice.

GRAPHICAL ABSTRACT



ARTICLE INFO

Article history:

Received 5 April 2025

Revised 24 May 2025

Accepted 17 June 2025

Available online xxx

Keywords:

Type 2 Diabetes Mellitus

Cognitive dysfunction

ABSTRACT

Introduction: Cognitive dysfunction is a prevalent complication associated with Type 2 Diabetes Mellitus (T2DM). Cognitive dysfunction in patients with T2DM not only severely impacts their quality of life but also imposes a substantial burden on their families and society. Despite the increasing prevalence of T2DM and its associated cognitive dysfunction, the underlying mechanisms remain incompletely understood, and effective treatment strategies are still lacking. This creates an urgent need for in-depth research to clarify these mechanisms and develop novel therapeutic approaches.

Objectives: This study aims to investigate the ameliorating effects of dietary n-3 polyunsaturated fatty acids (n-3 PUFA) on diabetes-related cognitive dysfunction and its underlying mechanisms.

* Corresponding authors at: School of Public Health, Capital Medical University, No. 10, Xitoutiao, You'anmen Street, Fengtai District, Beijing 100069, China.

E-mail addresses: gxjinger@163.com (X. Guo), ylhmedu@126.com (L. Yuan).

¹ These authors contribute equally to the work.

<https://doi.org/10.1016/j.jare.2025.06.044>

2090-1232/© 2025 The Author(s). Published by Elsevier B.V. on behalf of Cairo University.

This is an open access article under the CC BY-NC-ND license (<http://creativecommons.org/licenses/by-nc-nd/4.0/>).

n-3 polyunsaturated fatty acid
Mitochondrial dysfunction
Energy metabolism

Methods: In this study, we employed multiple mouse models of diabetes and cognitive impairment to explore the impact of disrupted glucose metabolism on central insulin signaling pathways and mitochondrial function. Furthermore, we treated db/db mice with n-3 PUFA-enriched diets and assessed the effects of n-3 PUFA on insulin signaling pathways, mitochondrial function, and cognitive function to elucidate the mechanisms by which n-3 PUFA mitigate diabetes-related cognitive dysfunction. The expression levels of target proteins and genes were detected using western blot, immunohistochemistry, and reverse transcription-polymerase chain reaction. Cognitive function was evaluated using the Morris water maze test, while damage of brain structure and neurons was analyzed through diffusion tensor imaging and Nissl staining. Mitochondrial morphology was examined by transmission electron microscopy, and energy metabolism alterations were investigated using metabolomics.

Results: db/db mice exhibited pronounced insulin resistance and mitochondrial dysfunction in the brain cortex. Abnormalities in brain mitochondrial energy metabolism and disruptions in the glutamate-glutamine circulation constitute the pathological basis for diabetes-related cognitive dysfunction. Dietary n-3 PUFA intervention alleviated insulin resistance, neuronal loss, mitochondrial structural abnormalities, energy metabolism disorders, glutamate-glutamine cycling disorders and cognitive dysfunction in db/db mice.

Conclusion: n-3 PUFA facilitated the recovery of cognitive function in T2DM mice by regulating cortical mitochondrial energy metabolism and enhancing the glutamate-glutamine cycle.

© 2025 The Author(s). Published by Elsevier B.V. on behalf of Cairo University. This is an open access article under the CC BY-NC-ND license (<http://creativecommons.org/licenses/by-nc-nd/4.0/>).

Introduction

Type 2 Diabetes Mellitus (T2DM), characterized by hyperglycemia, insulin resistance, and progressive pancreatic β -cell dysfunction, is strongly linked to cognitive dysfunction, which seriously impacts the management quality in T2DM patients [1]. T2DM doubles the risk of all-cause dementia, including Alzheimer's Disease (AD) and other forms of dementia [2], with abnormal glucose metabolism and insulin resistance identified as key drivers [3]. Furthermore, individuals diagnosed with AD exhibit disturbances in insulin signaling pathways, characterized by aberrant activation of proteins such as Insulin Receptor (IR), insulin-like growth factor 1 receptor (IGF-1R), and insulin receptor (IRS), alongside diminished brain sensitivity to insulin [4–6]. Positron emission tomography (PET) studies have revealed that among older adults with normal cognitive function, those with higher Homeostasis Model Assessment-Insulin Resistance (HOMA-IR) scores demonstrate reduced brain glucose metabolism [7]. In rodent models, glucose-induced neurotoxicity and disruptions in insulin signaling pathways can impair the structure and function of the brain, leading to behavioral and cognitive dysfunction [8,9].

Mitochondrial dysfunction is a shared pathological alteration in both T2DM and cognitive dysfunction. It disrupts energy supply and induces oxidative stress, both of which impair synaptic plasticity and neurotransmitter homeostasis [10–12]. Insulin resistance impairs brain glucose metabolism and mitochondrial dysfunction, bridging AD and T2DM [13]. Mice with diabetes mellitus and impaired cognitive function display reduced efficiency of the tricarboxylic acid cycle (TCA) in the hippocampus, cortex, and striatum [14]. The intermediates of the TCA cycle, including citric acid and succinic acid, can also be observed to undergo a significant reduction in threat hippocampus [8]. Furthermore, antidiabetic medications, such as rosiglitazone, can improve brain glucose metabolism and mitochondrial respiratory function in patients with early-stage diabetes, thereby lowering the incidence of cognitive dysfunction associated with the condition [15,16]. However, the central insulin signaling and mitochondrial changes in abnormal glucose metabolism, especially when combined with AD, remain understudied.

n-3 polyunsaturated fatty acid (n-3PUFA) have shown promise in the management of T2DM, particularly in regulating glycosylated hemoglobin (HbA1c) levels in diabetic patients [17]. An increased dietary intake of n-3 PUFA can enhance insulin sensitivity and is more conducive to controlling blood glucose levels in

T2DM patients, thereby reducing the risk of T2DM and dementia [18]. Low dietary docosahexaenoic acid (DHA) intake is associated with cognitive decline, and reduced plasma DHA levels are linked to hippocampal atrophy and amyloid beta protein ($A\beta$) deposition [19]. However, it remains unclear whether n-3 PUFA intake can restore diabetes-related cognitive dysfunction by improving central mitochondrial function remains unclear. Current research gaps exist in understanding how interventions targeting metabolic pathways impact brain mitochondrial function and energy metabolism under abnormal glucose conditions. This leaves a crucial aspect of understanding and potentially treating diabetes – associated cognitive decline unexplored.

This study initially investigated the central insulin signaling pathway and mitochondrial function of mice with abnormal glucose metabolism in different cognitive functional states. Subsequently, we used db/db mice as the T2DM model to explore the effects and mechanisms of dietary n-3 PUFA intervention in ameliorating diabetes-related cognitive dysfunction, focusing on alterations in brain mitochondrial function and energy metabolism.

Material and methods

Experimental animals

Male C57BL/6J, db/db and APP/PS1 mice were purchased from Cyagen biotechnology Co., Ltd. Animals were housed in Capital Medical University's animal facility under controlled conditions: 24–29°C temperature, 50–60% humidity, 15–20 lx light intensity, 12-h light–dark cycle, with free access to water.

After a week of adaptation, mice were randomly grouped (10 mice per group) based on fasting blood glucose and baseline weight for dietary intervention. The mouse intervention study in this study consisted of the following three parts (detailed composition of the feed are in the [supplementary materials](#)):

- i. C57BL/6J mice were fed with control diet, while APP/PS1 mice were divided into two groups: the APP group, which consisted of APP/PS1 mice fed with a control diet, and the APP HFD group, which consisted of APP/PS1 mice fed with a high-fat diet to establish an insulin resistance model combined with Alzheimer's Disease (AD). After 7 months of feeding, samples were taken and corresponding indicators were tested.

- ii. C57BL6/J mice were divided into two groups: one served as the control group and was fed a control diet, while the other group was fed a high-fat diet to induce insulin resistance. db/db mice were used as the diabetes model group and were also fed the control diet. After 3 months feeding, samples were taken and corresponding indicators were tested.
- iii. C57 RC group: C57BL6/J mice fed with a control diet, while db/db mice were randomly divided into three groups based on fasting blood glucose levels. db/db group: T2DM mice fed with a control diet; db/db LD group: T2DM mice fed with low dose n-3 PUFA feed, and db/db HD group: T2DM mice fed with high dose n-3 PUFA feed. After 3 or 6 months feeding, samples were taken and corresponding indicators were tested.

Fasting blood glucose (FBG) measurement

Mice fasted for 12 h (with water access) and tail-vein blood was collected monthly using an ACCU-CHEK® Performa device to monitor fasting glucose levels.

Morris water maze

After a week of adaptation in the testing room, the test was conducted in circular tank with a diameter of 120 cm and a height of 40 cm, featuring a platform located in the third quadrant. (Beijing Zhongshi Dichuang Technology Development Co., Ltd.). According to the previously described methods [20], the positioning navigation lasted 4 days. On the fifth day, a spatial exploration experiment was conducted with the platform removed. Escape latency and platform crossings were analyzed.

Blood collection and separation of brain tissue

After intervention, mice fasted for 12 h and were anesthetized with 2.5 % Avertin (ip.). 2–3 ml of blood was collected from the eyeball into anticoagulant tubes. Mice were euthanized by decapitation, and organs and brain tissue were dissected. Tissues were rinsed with 0.9 % saline, dried, and weighed. Half of the brain tissues were fixed in 4 % paraformaldehyde at room temperature, and the rest was stored at –80°C. Blood was centrifuged (3000 rpm, 15 min) to collect plasma.

Western blot analysis

Samples were weighed, and radio immunoprecipitation assay (RIPA) lysis buffer (1:10 wt: volume), 1 % phosphatase inhibitor, and 1 % phenylmethylsulphonyl fluoride (PMSF) were added. Protein concentration was determined using a kit (New Cell & Molecular Biotech Co., Ltd). Loading buffer was added (4:1), and samples were incubated at 100 °C. Sodium dodecyl sulfate–polyacrylamide gel electrophoresis (SDS-PAGE) was done, and proteins were transferred to a polyvinylidene fluoride (PVDF) membrane. The membrane was blocked with 5 % skim milk (Beyotime Biotechnology Co., Ltd), incubated with the primary antibody at 4°C overnight, washed with tris buffer saline (TBST), and then incubated with fluorescent secondary antibody for 1 h. Bands were scanned (Odyssey CLx) and analyzed with Image J software. Antibody details are in [Supplementary Table 3](#).

Reverse transcription-polymerase chain reaction (RT-PCR)

RNA was extracted following the kit (FastPure® Cell/Tissue Total RNA Isolation Kit V2, Vazyme, RC112) guidelines. cDNA was synthesized using the kit (HiScript® III RT SuperMix for qPCR, Vazyme, RC323). Primers for target gene were from National Center for

Biotechnology Information (NCBI)-gene website, designed with SnapGen software, and validated on NCBI-Blast. Application followed the instructions (Taq Pro Universal SYBR qPCR Master Mix). GAPDH was the internal reference, and relative expression was calculated using the $2^{-\Delta\Delta Ct}$ method. Primers sequences are in [Supplementary Table 4](#).

Immunohistochemistry (IHC)

According to the previously described methods [21], paraffin-embedded brain tissue sections were assayed with antibodies against heat shock protein 60 (HSP60) (1:2000 dilution; Abcam, UK) and glial fibrillary acidic protein (GFAP) (1:1200 dilution; Abcam, UK). A secondary DAB antibody was used for detection. The sections were scanned with Panoramic SCAN system, and positive staining was quantitatively assessed using ImageJ software.

Nissl staining

Prepare slices according to previous descriptions [22]. Three fields of view from the cortex and hippocampus were selected for photography and cell counting with Image J software.

Hematoxylin-eosin staining

Prepare slices according to previous descriptions [23]. Sections were scanned with Panoramic SCAN system, and assessed with ImageJ software.

Oil red O staining

Prepare slices according to previous descriptions [23]. Sections were scanned with Panoramic SCAN system, and assessed with ImageJ software.

Transmission electron microscope

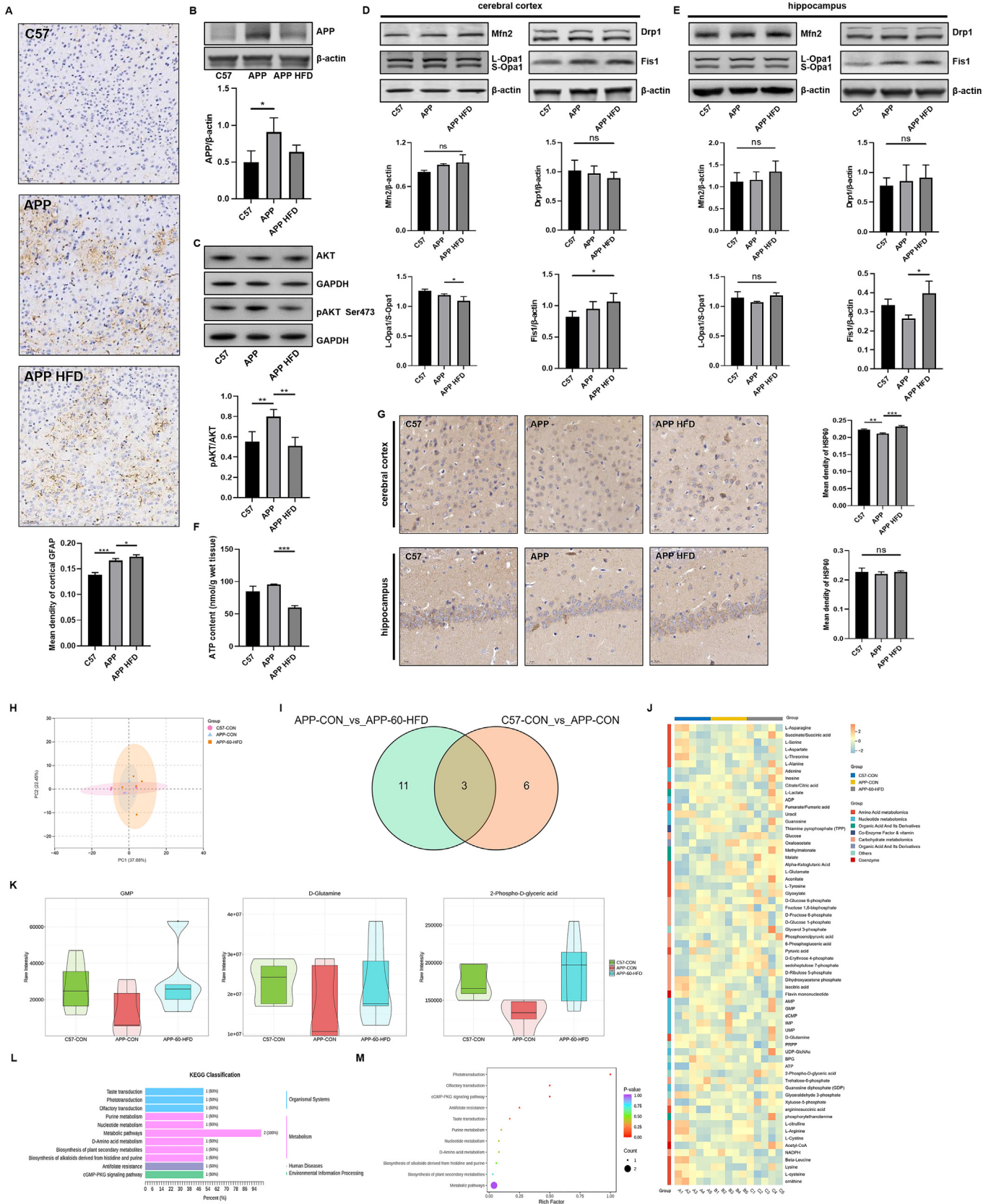
Freshly isolated cortex and hippocampus tissues (1 mm³ cubes) were fixed in 2.5 % glutaraldehyde at 4°C overnight, washed with 0.1 M phosphate buffer, and sent to Core Facilities Center of Capital Medical University. Ultrastructural analysis was performed with a transmission electron microscope (JEOL, JEM-2100, JPN), and representative images were captured.

Diffusion tensor imaging (DTI)

According to the previously described methods [24], brain DTI was performed using a small animal MRI system (Bruker, PharmaScan 7.0/16 US, GER) at the Core Facilities Center of Capital Medical University.

Targeted energy metabolomics

UPLC-MS/MS was used to analyze brain differential metabolites in mice. 50 mg of tissue was extracted with 500 µl of 70 % methanol in water internal standard extraction solution. After homogenization and shaking, the supernatant was analyzed. Liquid phase conditions included column (SeQuant ZIC-pHILIC 5 µm, 2.1 × 100 mm), mobile phase, elution gradient, etc. Mass spectrometry settings were also defined. Data was analyzed with R 4.2.1 software, and characterized with OPLS-DA. Differential metabolites were screened based on VIP, *p*-value, and fold change ($FC \geq 1.2$ or $FC \leq 0.83$, $VIP > 1$, and $P < 0.05$).



Quantification of assay kit

Indicator concentrations were quantified using assay kits according to the instructions. Detailed information is in [Supplementary Table 5](#).

Statistical analysis

SPSS 25.0, R 4.2.1 and GraphPad Prism 8.0 were used. Measurement data were presented as $M \pm SD$. Normality and variance homogeneity were tested before intergroup comparison. One-way ANOVA test and LSD method were used for normal data, and Kruskal-Wallis test followed by Dunnett method for non-normal data. $P \leq 0.05$ was indicated statistically significant.

Results

The effect of high-fat diet on central inflammation and AD pathology in APP/PS1 mice

After a 7-month dietary intervention, APP HFD group exhibited a significant increase in body weight compared to the APP group ($P < 0.05$, [Supplementary Fig. 1A](#) and B). The cortical GFAP+ regions in the APP group were increased compared with the C57 group, and the cortical GFAP intensity in APP HFD group was higher than that in the APP group ($P < 0.05$, [Fig. 1A](#)). We investigated the expression of AD-associated pathological proteins in the cortex and hippocampus of these mice. The expression of APP protein in the cortex of APP/PS1 mice was higher than that of C57 mice ($P < 0.05$, [Fig. 1B](#)).

The effect of high-fat diet on insulin signaling pathway related proteins in cortex and hippocampus of APP/PS1 mice

As shown in [Fig. 1C](#), the cortical pAKT/AKT ratio in the APP group of mice was higher than that in both the C57 group and the APP-HFD group ($P < 0.05$). However, the pathological status of AD and HFD intervention did not affect the expression and activation of Insulin Receptor (IR), insulin receptor substrate (IRS1), and glycogen synthase kinase-3 (GSK3 β) proteins in the brain of APP/PS1 mice ([Supplementary Fig. S1](#)).

The effect of high-fat diet on mitochondrial function in APP/PS1 mice

We observed that the mitochondrial fusion protein optic atrophy factor 1 (L-Opa1/S-Opa1) ratio in cortex was reduced in the APP HFD group compared to the APP group, but the expression of

mitochondrial fission protein Fis1 was increased in the hippocampus ($P < 0.05$, [Fig. 1D](#) and E). The adenosine triphosphate (ATP) level in the cortex of the APP HFD group was lower than that of the APP group ($P < 0.05$, [Fig. 1F](#)). Additionally, the expression levels of the heat shock proteins (HSP60), a mitochondrial molecular chaperone, were higher in the cortex of C57 and APP HFD mice compared with the APP group ($P < 0.05$, [Fig. 1G](#)).

Targeted energy metabolomics analysis of hippocampus

64 Metabolites involved in energy metabolism were detected after stable quality control ([Fig. 1H](#)). There were 14 differential metabolites between the APP group and the C57 group, and 9 differential metabolites were found between the APP HFD group and the APP group ([Fig. 1I](#)). The shared three differential metabolites among groups involved in metabolic pathways, including guanosine 5'-monophosphate (GMP), D-glutamine, and 2-phosphate-D-glyceric acid, were decreased in APP group compared with C57 group and APP HFD group ([Fig. 1J–M](#), [Fig. 1K](#)).

The effect of abnormal glucose metabolism on central inflammation and AD pathology in mice

At the end of the dietary intervention, body weight gain was observed ($P < 0.05$, [Supplementary figure S2](#)). The GFAP+ region was increased in the cerebral cortex of mice in the HFD group and the db/db group compared with that in the C57 group ($P < 0.01$, [Fig. 2A](#) and B). The expression levels of β -site APP cleaving enzyme 1 (BACE1) and APP proteins in the cortex were higher in the HFD group compared to the C57 group, and the expression of BACE1 proteins in hippocampus were lower in the db/db group than that in the control C57 group ($P < 0.05$, [Fig. 2C](#) and D). In addition, the p-tau/tau ratio of both cerebral cortical and hippocampal were higher in the db/db mice than in the C57 mice ($P < 0.05$, [Fig. 2C](#) and D).

Expression and activation of cortical and hippocampal insulin signaling pathway proteins in mice

The cortical pIR/IR ratio was elevated in the db/db group compared with the C57 group, and the cortical pIRS1/IRS1 ratio was also higher in both the HFD group and db/db group compared with the C57 group ($P < 0.001$, [Fig. 2E](#) and F). Furthermore, db/db mice showed an increased cortical pAKT/AKT ratio and pGSK3 β /GSK3 β ratio compared with the C57 group ($P < 0.05$, [Fig. 2E](#) and F).

Fig. 1. The effect of high-fat diet on central inflammation, AD pathology, mitochondrial function and hippocampal energy metabolomics in APP/PS1 mice. A: Representative images and quantitative data for GFAP expression in the cortex of each group (n = 3, 40 \times); B: Representative protein bands and quantitative analysis of APP in the cortex of mice (n = 5); C: Representative protein bands and quantitative analysis of p-AKT ser473/AKT in the cortex of mice (n = 5); D-E: Representative protein bands and quantitative analysis of mitochondrial fusion proteins (Mfn2, L-Opa1/S-Opa1) and fission proteins (Drp1, Fis1) in the cortex (D) and hippocampus (E) of mice (n = 5); F: Cortical ATP content in each group (n = 5); G: Representative images and quantification results of cortical HSP60 for each group in the cortex and hippocampus of mice (n = 3, 40 \times); H: Principal component analysis (PCA) graph of different groups, the distribution of different groups of samples in omics data was demonstrated, and the differences and similarities of metabolites between different groups of samples were reflected through PCA analysis (n = 5); I: Venn diagrams comparing "APP – CON vs APP – 60 – HFD" and "C57 – CON vs APP – CON", the numbers represent the number of shared and unique differentially expressed metabolites between different groups, used to analyze the overlap relationship of differentially expressed metabolites between different comparison groups (n = 5); J: Heatmap, analysis was conducted on different substances in different samples, and the color intensity was used to indicate the level of content, visually displaying the difference patterns between different samples; K: Violin diagram of GMP, D – Glutamine and 2-phosphate-D-glycolic acid levels among different groups, the distribution of metabolites in different groups was displayed to compare the differences in data distribution between different groups. (n = 5); L-M: KEGG enrichment classification, and statistically analyze the detected metabolites according to different functional categories, reflecting the distribution of metabolite functions. (n = 5). AD, Alzheimer's Disease; GFAP, Glial Fibrillary Acidic Protein; APP, Amyloid Precursor Protein; BACE1, β -Site App Cleaving Enzyme 1; AKT, Protein Kinase; HFD, High Fat Diet; Opa1, Optic Atrophy Factor 1; Fis1, Mitochondrial Fission Protein 1; Drp1, Dynamin Related Protein 1; Mfn2, Mitochondrial Fusion Proteins 2; ATP, Adenosine Triphosphate; HSP60, Heat Shock Protein 60. ns: no statistical difference, * $P < 0.05$, ** $P < 0.01$, *** $P < 0.001$.

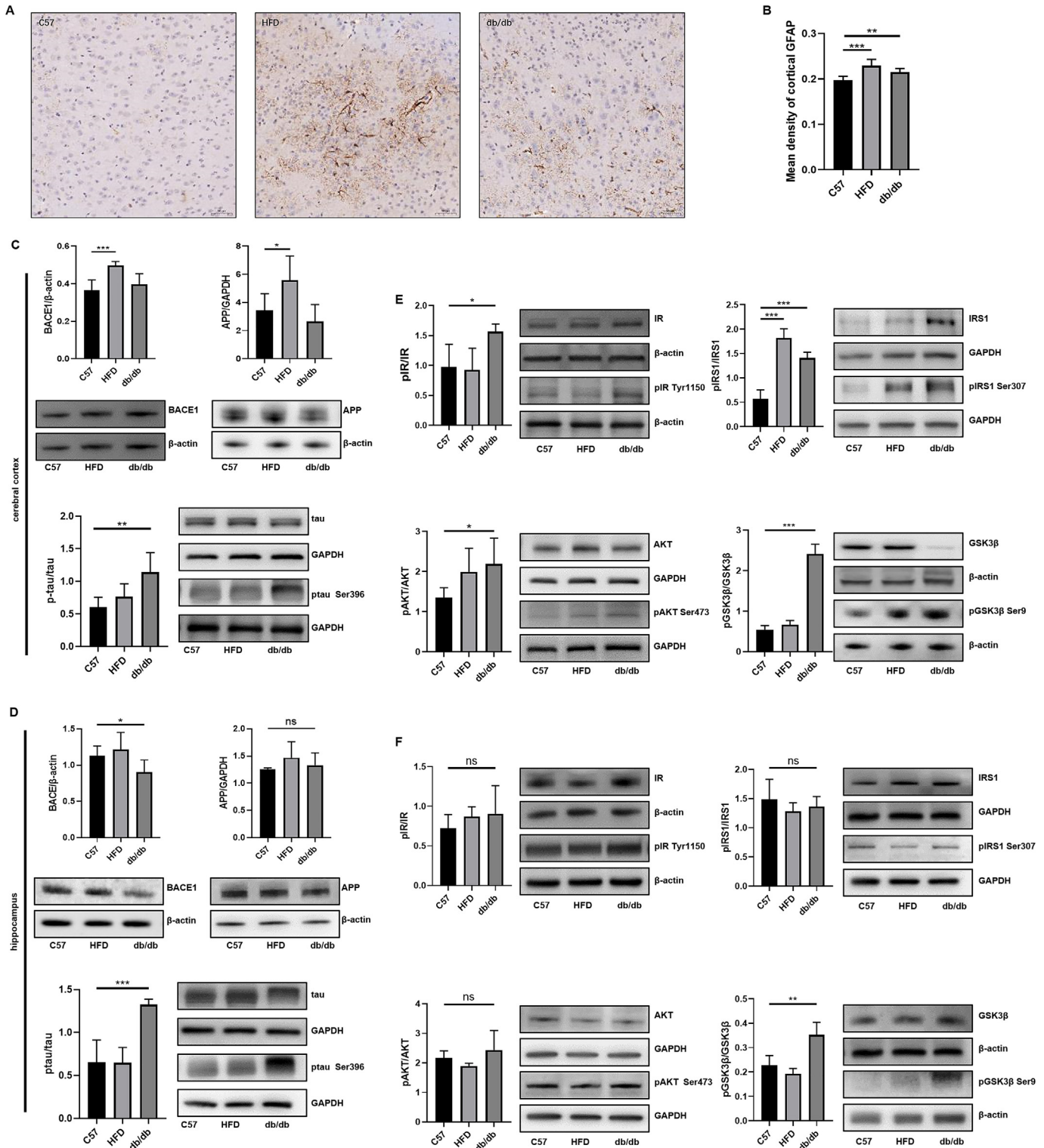


Fig. 2. Inflammation, AD pathological and insulin signaling pathway molecules in brain of mice with abnormal glucose metabolism. A-B: Representative images and quantitative results of cortical GFAP in each group ($n = 3, 40 \times$); C: Representative protein bands and quantitative analysis of APP, BACE1 and p-tau/tau in the cortex of mice ($n = 5$); D: Representative protein bands and quantitative analysis of APP, BACE1 and p-tau/tau in the hippocampus of mice ($n = 5$); E: Representative protein bands and quantitative analysis of insulin signaling pathway proteins (IR, IRS1, AKT, GSK3 β) and phosphorylated proteins (p-IR Tyr1150, p-IRS1 ser307, p-AKT ser473, p-GSK3 β ser9) in the cortex of mice ($n = 5$); F: Representative protein bands and quantitative analysis of insulin signaling pathway proteins (IR, IRS1, AKT, GSK3 β) and phosphorylated proteins (p-IR Tyr1150, p-IRS1 ser307, p-AKT ser473, p-GSK3 β ser9) in the hippocampus of mice ($n = 5$). AD, Alzheimer's Disease; GFAP, Glial Fibrillary Acidic Protein; APP, Amyloid Precursor Protein; BACE1, β -Site App Cleaving Enzyme 1; IR, Insulin Receptor; IRS1, Insulin Receptor Substrate; GSK3, Glycogen Synthase Kinase-3AKT, Protein Kinase B. ns: no statistical difference, * $P < 0.05$, ** $P < 0.01$, *** $P < 0.001$.

Mitochondrial function changes in the cortex and hippocampus of mice with abnormal glucose metabolism

As depicted in Fig. 3A–D, the expression level of the cortical mitochondrial fusion proteins 2 (Mfn2) in the db/db group was lower than that in the C57 group ($P < 0.05$). Compared with the C57 group, the expressions of cortical dynamin-related protein 1 (Drp1) and Fis1 were upregulated in db/db mice, and the expression of Fis1 protein in the hippocampus was consistently ($P < 0.05$, Fig. 3A–D). In the cortex of db/db mice, the expression level of HSP 60 was lower compared to that in C57 mice, whereas the hippocampus exhibited the opposite result ($P < 0.05$, Fig. 3E and F).

Quantitative analysis of cortical ATP levels revealed a significant reduction in db/db mice compared to C57 mice ($P < 0.05$, Fig. 3G). In addition, the expression level of NDUFB8 protein in the HFD group was higher compared to that in the C57 group, and the expression of the ATP5A protein was higher in the db/db group than in the C57 group ($P < 0.05$, Fig. 3H and I).

The effect of n-3 PUFA on the growth and peripheral glucose metabolism of db/db mice

During the dietary intervention, all db/db mouse groups demonstrated a significant increase in the body weight compared to the C57 RC group ($P < 0.05$, Supplementary Fig. S3A and B). The fasting blood glucose and HOMA-IR index of the db/db mice were higher than that of C57 mice ($P < 0.05$, Fig. 4A and B). After a 3-month intervention, the fasting plasma insulin levels in db HD mice were higher than those of the db RC group. Moreover, compared to the db/db mice received 3-month intervention, the mice treated with 6-month high-dose n-3 PUFA intervention showed a decrease in the fasting plasma insulin levels ($P < 0.05$, Fig. 4C).

The pancreas of db/db mice were severely damaged, exhibiting irregular shapes and a disordered arrangement of cells. There was obvious vacuolization in the cytoplasm, and the entire pancreas appeared visibly swollen. After intervention with a low-dose n-3 PUFA diet, compared to the db RC group, the pancreas structure of db/db mice showed significant improvement. However, obvious swelling and vacuolization were still observable. Moreover, after intervention with a high-dose n-3 PUFA diet, there were no obvious swelling or vacuolization, and β cells arranged more closely (Fig. 4D).

The db/db mice exhibited significant hepatic pathological changes, mainly manifested as severe vacuolation of hepatocytes, extensive lipid deposits, and disordered cell arrangement (Fig. 4E–G). In comparison to the db RC group, the liver lesions in the db LD and db HD groups were notably ameliorated. The hepatocytes displayed a more organized arrangement, the cellular morphology approached normalcy, and lipid accumulation was reduced after intervention. In addition, these improvements were more pronounced after intervention with a high-dose n-3 PUFA diet.

The effect of n-3 PUFA on cognitive function and AD pathology in db/db mice

In the location navigation experiment, the escape latency of db/db mice was longer than that of C57 mice. After 6 months of dietary intervention, the escape latency of db HD mice was shorter than that of db RC mice ($P < 0.05$, Fig. 5A and B). The number of cortical neurons in db RC mice was fewer than that in C57 RC mice ($P < 0.05$). After 3 months of intervention, cortical neuron count increase in db LD and db HD mice compared to db RC mice ($P <$

0.05 , Fig. 5C and D). After 6 months of dietary intervention, the hippocampal neuron loss was reduced significantly in n-3 PUFA fortified diets-fed db/db mice ($P < 0.05$, Fig. 5E and F).

The effect of n-3 PUFA on the cortical insulin signaling pathway in db/db mice

Compared to the db LD mice treated with n-3PUFA intervention for 3 months, the mice treated with intervention diets for 6 months showed increased cortical insulin levels ($P < 0.05$, Fig. 5G). After 3 months of dietary intervention, the expression level of cortical insulin I mRNA in db RC mice was significantly higher than that in C57 RC mice. In contrast, both db LD and db HD groups showed downregulated insulin I mRNA expression compared to the db RC group. Additionally, extended intervention with high-dose n-3 PUFA for 6 months significantly attenuated insulin I mRNA expression in db/db mice ($P < 0.05$, Fig. 5H).

Following the 3 months of dietary intervention, both the cortical pAKT/AKT and pGSK3 β /GSK3 β ratios were significantly elevated in db RC mice compared to C57 mice ($P < 0.05$, Fig. 5I and J). Moreover, the pGSK3 β /GSK3 β ratio in the cortex of db HD mice was notably higher than that of db RC mice ($P < 0.05$, Fig. 5I and J). After 6 months of control diet feeding, db/db mice exhibited a significant increase in the cortical pIRS1/IRS1 ratio but a reduction in the pAKT/AKT ratio compared to C57 mice ($P < 0.05$, Fig. 5K and L). Furthermore, following a high-dose n-3 PUFA dietary intervention, the cortical pAKT/AKT ratio and pGSK3 β /GSK3 β ratio in db HD mice were increased compared to the db RC group ($P < 0.05$, Fig. 5K and L).

The effect of n-3 PUFA on cortical mitochondrial function in db/db mice

As shown in Fig. 6A, the mitochondria within the cytoplasm of cortical neurons from C57 mice exhibited a normal morphological structure, characterized by an intact double-membrane structure, distinct cristae and closely packed cristae. In contrast, the mitochondria of cortical neurons from db/db mice displayed evident structural damage, including severe swelling and vacuolization of the mitochondria, extensive disruption of cristae and the cristae space disappeared. The protective effect of n-3 PUFA on mitochondrial structural integrity in db/db mice exhibited a dose-dependent response. Mitochondrial swelling in the db LD group was marginally alleviated, yet obvious damage persisted. The mitochondrial structure in the db HD group approached normalcy, with no pronounced swelling and the inner mitochondrial cristae being closely arranged.

After 6 months of dietary intervention, the expression level of the cortical Fis1 protein in the db LD mice was significantly higher than that in db RC mice ($P < 0.05$, Fig. 6E). The activity of mitochondrial complex V in the cortex of db/db mice was significantly higher than that of C57 mice after intervention ($P < 0.05$, Fig. 6F). Additionally, after 3 months of dietary intervention, the activity of complex V in the db HD mice was lower than that of db RC and db LD mice. After 6 months of dietary intervention, both db LD and db HD mice exhibited significantly reduced complex V activity compared to db RC mice, and the activity of complex V decreased with increasing age of mice ($P < 0.05$, Fig. 6F and G). The cortical ATP content in db LD mice was significantly increased in comparison with db/db mice. Notably, db/db mice maintained higher cortical ATP levels than C57 mice throughout the study period, and this elevation persisted in db LD mice after 6 months of intervention compared to db RC mice ($P < 0.05$, Fig. 6H). Moreover, as age increased in mice, the cortical ATP level decreased conversely ($P < 0.05$, Fig. 6I).

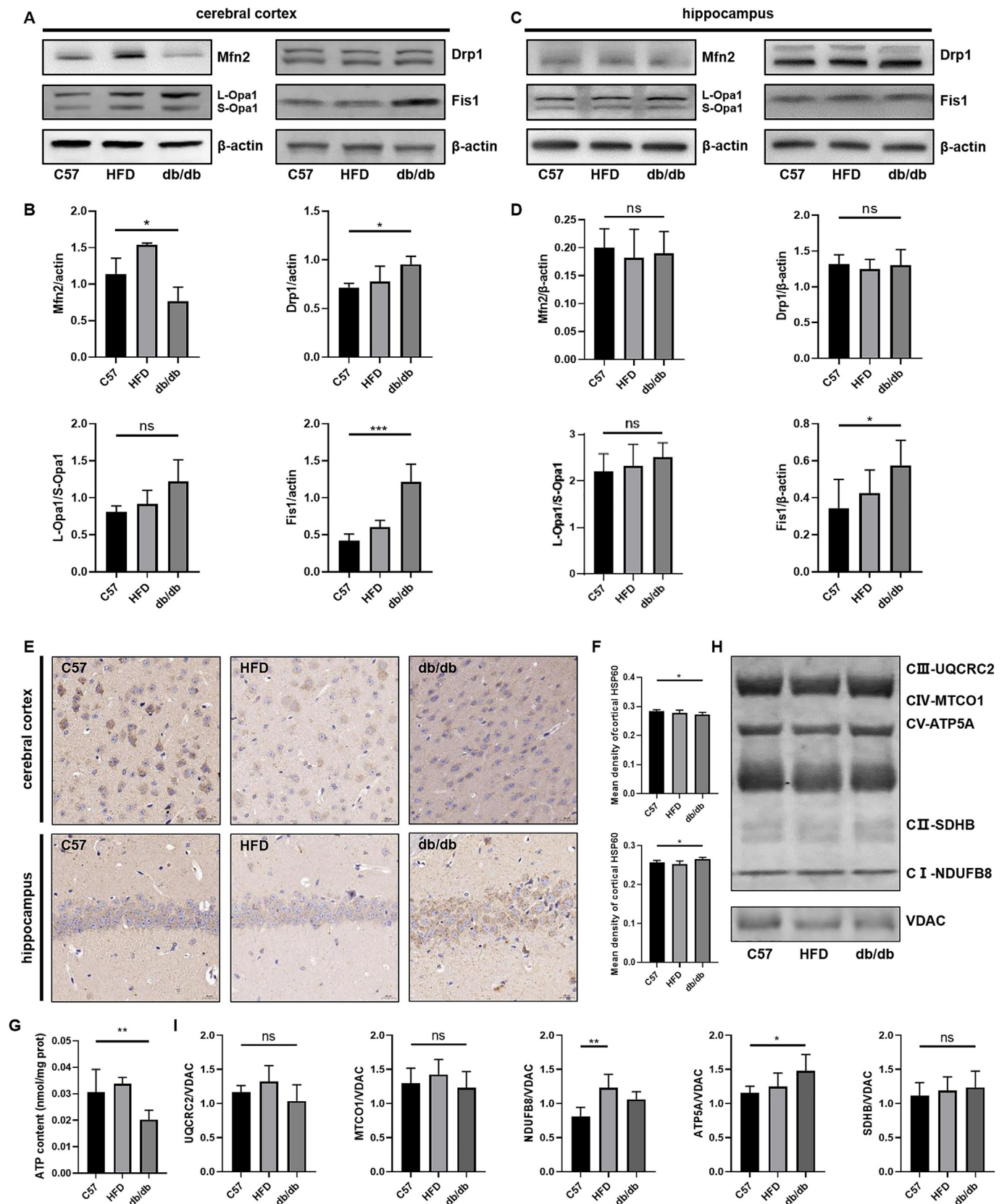


Fig. 3. Changes in mitochondrial function in the cortex and hippocampus of mice with abnormal glucose metabolism. A-D: Representative protein bands and quantitative analysis of mitochondrial fusion proteins (Mfn2, L-Opa1/S-Opa1) and fission proteins (Drp1, Fis1) in the cortex (A-B) and hippocampus (C-D) of mice (n = 5); E-F: Representative images and quantitative results of HSP60 in cortex and hippocampus of mice (n = 3, 40 ×); G: Cortical ATP content in each group (n = 5); H-I: Representative protein bands and quantitative analysis of mitochondrial respiratory chain complexes in the cortex (CIII-UQCRC2, CIV-MTCO1, CI-NDUFB8, CV-ATP5A, CII-SDHB) (n = 5). Opa1, Optic Atrophy Factor 1; Fis1, Mitochondrial Fission Protein 1; Drp1, Dynamin Related Protein 1; Mfn2, Mitochondrial Fusion Proteins 2; ATP, Adenosine Triphosphate; HSP60, Heat Shock Protein 60; NDUFB8, NADH: Ubiquinone Oxidoreductase Subunit B8; ATP5A, ATP Synthase F1 Subunit Alpha; UQCRC2, Ubiquinol-Cytochrome C Reductase Core Protein 2; MTCO1, Mitochondrially Encoded Cytochrome C Oxidase I; SDHB, Succinate Dehydrogenase Complex Iron Sulfur Subunit B. ns: no statistical difference, *P < 0.05, **P < 0.01, ***P < 0.001.

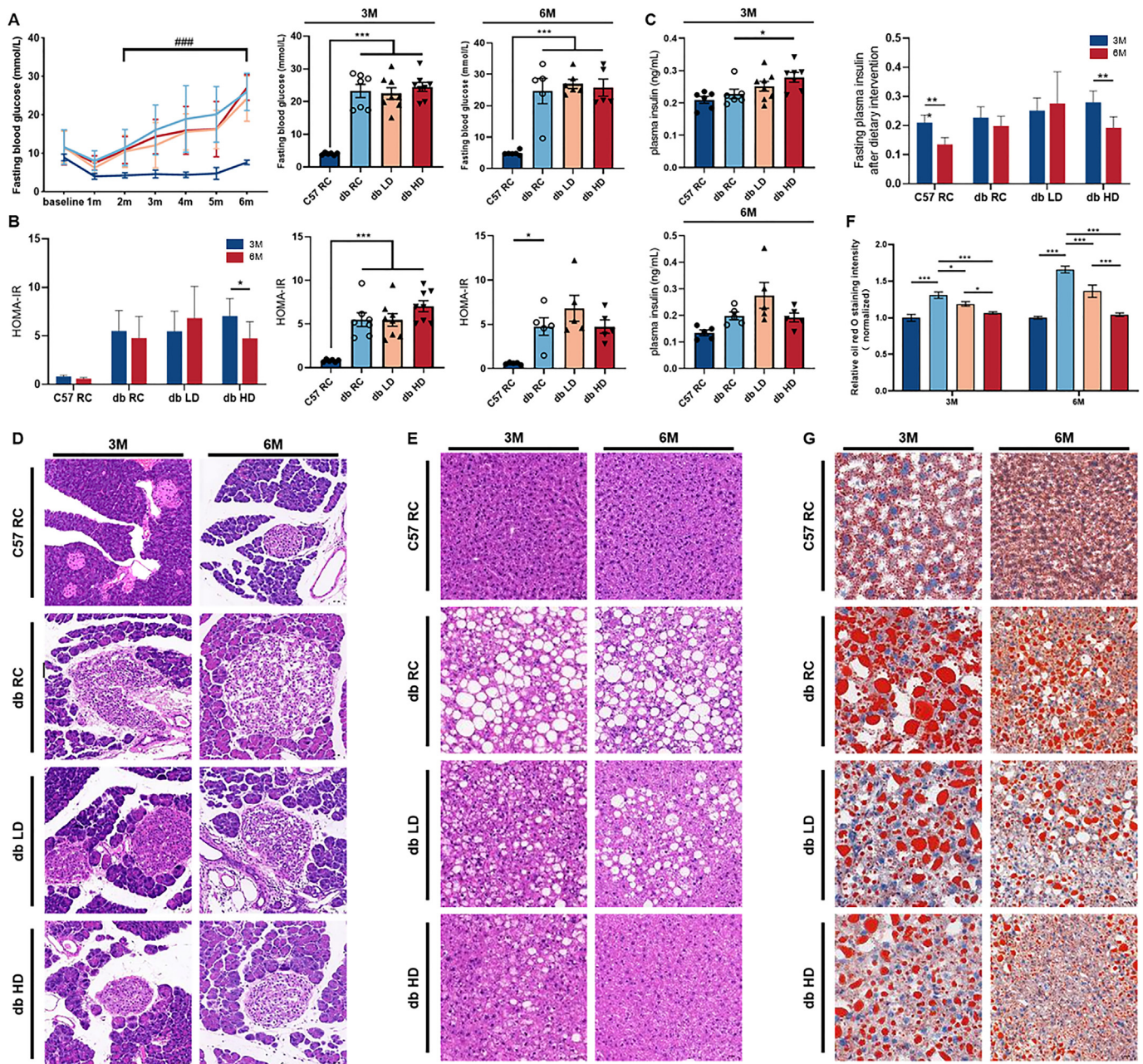


Fig. 4. The effects of n-3 PUFA intervention on the growth and diabetes pathology of db/db mice. A: Changes in fasting blood glucose levels after 3 and 6 months of dietary intervention in C57 and db/db mice ($n = 6-8$); B: HOMA-IR indexes after 3 and 6 months of dietary intervention in each group ($n = 6-8$); C: Plasma insulin levels of mice in each group after 3 and 6 months of dietary intervention ($n = 5-6$); D: HE staining images of the pancreas in each group after dietary intervention ($n = 3, 20 \times$); E: HE staining images of liver in each group after dietary intervention ($n = 3, 20 \times$); F-G: Oil Red O staining and quantification of liver in each group after dietary intervention ($n = 3, 20 \times$). n-3 PUFA, N-3 Polyunsaturated Fatty Acids; HOMA-IR, Homeostasis Model Assessment-Insulin Resistance; HE, Hematoxylin-Eosin Staining. ns: no statistical difference, $*P < 0.05$, $***P < 0.001$, $##P < 0.001$ vs. C57 RC. (For interpretation of the references to color in this figure legend, the reader is referred to the web version of this article.)

The effect of n-3 PUFA on cortical energy metabolism and glutamate-glutamine cycle in db/db mice

As shown in Fig. 6J, after dietary intervention for 3 months, the total $NAD^+ + NADH$ content in db RC mice was higher than that in C57 RC mice. The $NAD^+ + NADH$ content and NAD^+ content in the cortex of db HD mice were lower than those in the db RC group ($P < 0.05$). As illustrated in Fig. 6K, after dietary intervention for 6 months, the $NAD^+ + NADH$ content, NAD^+ content, and $NAD^+ / NADH$ ratio in the cortex of db/db mice were lower than those of C57 mice. The total $NAD^+ + NADH$ content, NAD^+ content and $NAD^+ / NADH$ ratio of db LD mice were higher than those of db RC

and db HD mice, while the cortical $NADH$ content exhibited an opposite trend ($P < 0.05$).

As depicted in Fig. 6L, compared to the C57 mice, the cortical *Idh2* mRNA levels of db/db mice increased after a 3-month intervention. Moreover, following the 3-month high-dose n-3 PUFA dietary intervention, the mRNA levels of *Ogdh* and *Idh2* genes were down-regulated compared to the db RC and db LD groups ($P < 0.05$). Conversely, the expression of *Idh2* mRNA in the db RC group was lower than that in the C57 RC group after a 6-month intervention. And the expression of *Idh2* mRNA of db HD mice was notably higher compared to those in db RC mice and db LD mice ($P < 0.05$).

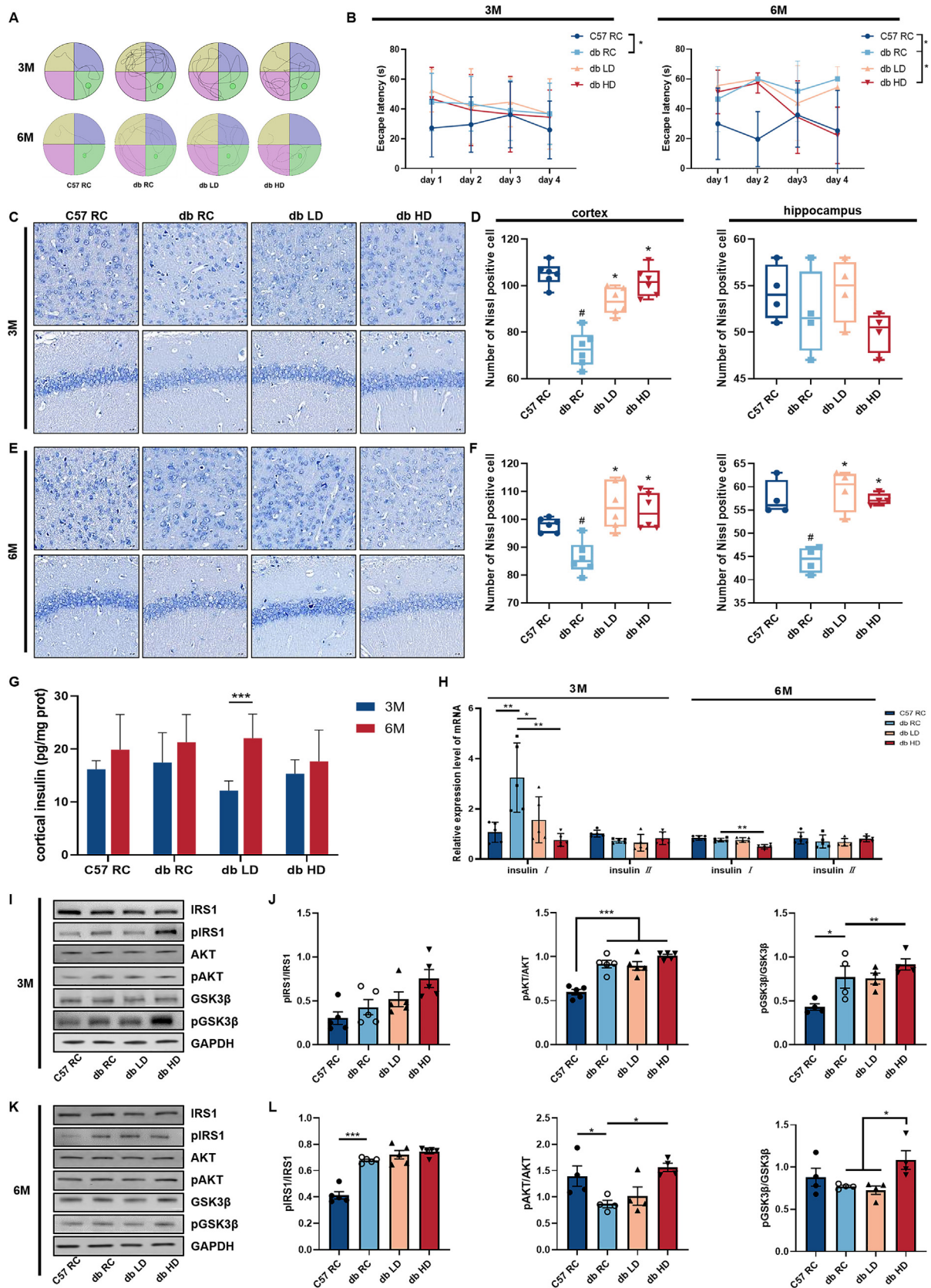


Fig. 5. The effects of n-3 PUFA on cognitive function, AD pathology and cortical insulin signaling pathway in db/db mice. A: Representative results of Morris Water Maze tests for mice in different feed groups and intervention times; B: The escape latency of mice in each group after 3 or 6 months of dietary intervention (n = 6–8); C–D: Representative images and quantitative results of Nissl staining in each group after 3 months of dietary intervention (n = 3, 40 ×); E–F: Representative images and quantitative results of Nissl staining in each group after 6 months of dietary intervention (n = 3, 40 ×); G: Insulin levels in the cortex of mice in different intervention groups (n = 5); H: Cortical insulin mRNA expressions in mice after dietary interventions (n = 5); I–L: Representative protein bands and quantitative analysis of insulin signaling pathway proteins (IRS1, AKT, GSK3β) and their phosphorylated forms (p-IR Tyr1150, p-IRS1 ser307, p-AKT ser473, p-GSK3β ser9) of mice (n = 5). n-3 PUFA, N-3 Polyunsaturated Fatty Acids; AD, Alzheimer's Disease; AKT, Protein Kinase B; IRS1, Insulin Receptor Substrate; GSK3, Glycogen Synthase Kinase-3. *P < 0.05, **P < 0.01, ***P < 0.001.

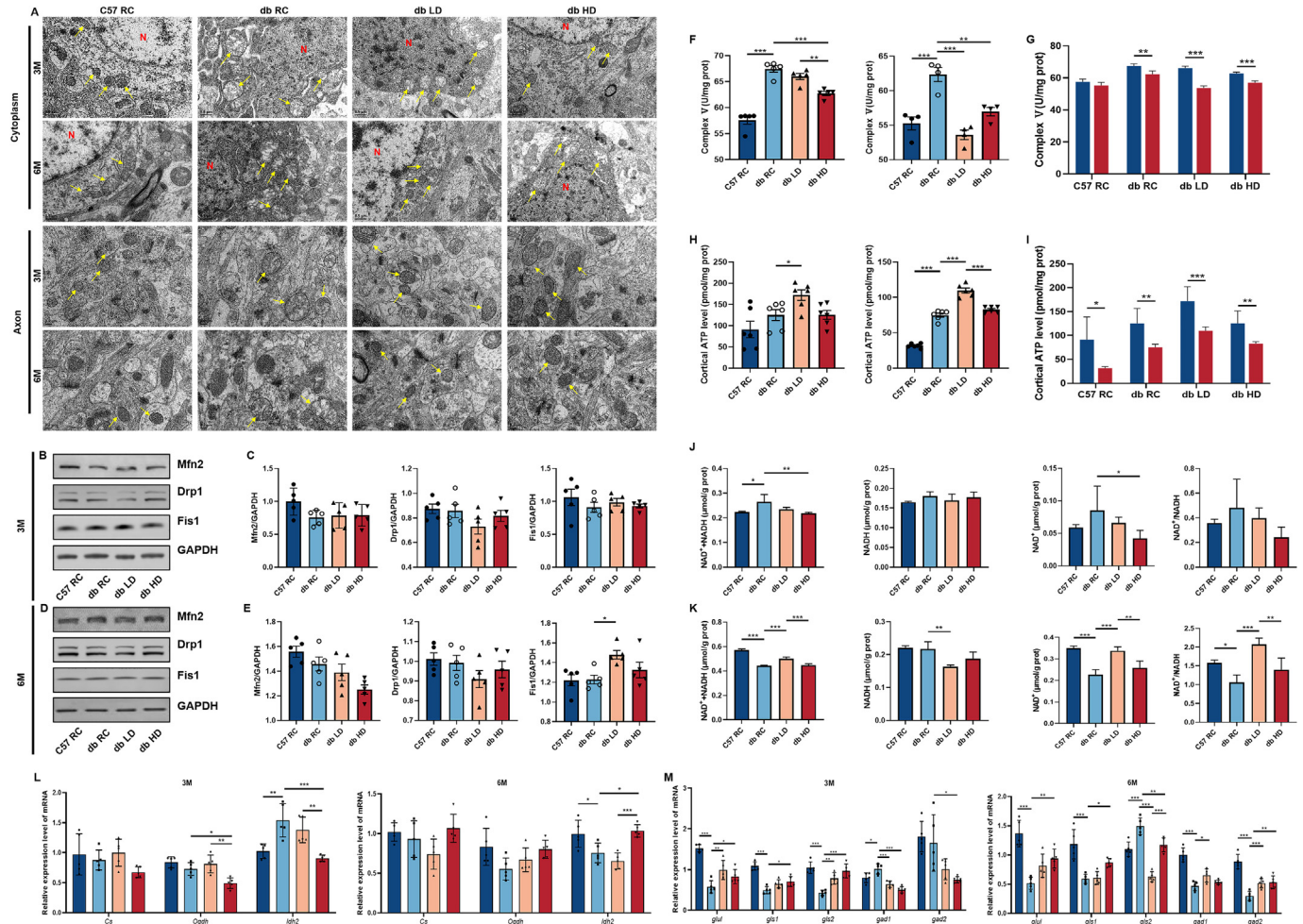


Fig. 6. Effects of n-3 PUFA on the structure and function of mitochondria, cortical energy metabolism and glutamate-glutamine cycle metabolism in cortex of db/db mice. A: Ultrastructural changes of mitochondria within the cytoplasm and axons of neurons in the cortex of mice after 3 or 6 months of dietary intervention (n = 3). N: nucleus; yellow arrows: mitochondria. B-E: Representative protein bands and quantitative analysis of mitochondrial fusion proteins (Mfn2) and fission proteins (Drp1, Fis1) of mice (n = 5); F-G: Mitochondrial respiratory chain complex V activity in the cortex of mice after 3-month (left) and 6-month (right) dietary interventions (n = 4–5), and comparison at different intervention times in each group (G); H-I: ATP content in the cortex of mice after 3-month (left) and 6-month (right) interventions (n = 6), and comparison at different intervention times in each group (I); J-K: Cortical NAD⁺, NADH content and the ratio in mice after 3-month (J) and 6-month (K) dietary interventions (n = 5); L: Expressions of Cs, Ogdh and Idh2 mRNA in the cortex of mice following 3-month and 6-month dietary interventions (n = 4–5); M: The mRNA levels of enzymes involved in the glutamate-glutamine cycle in the cortex of mice after 3-month and 6-month dietary interventions (n = 5). n-3 PUFA, N-3 Polyunsaturated Fatty Acids; Opa1, Optic Atrophy Factor 1; Fis1, Mitochondrial Fission Protein 1; Drp1, Dynamin Related Protein 1; Mfn2, Mitochondrial Fusion Proteins 2; ATP, Adenosine Triphosphate; Ogdh, Oxoglutarate Dehydrogenase; Idh2, Isocitrate Dehydrogenase; Glul, Glutamate-Ammonia Ligase; Cs, Citrate Synthase; Gls, Glutaminase; Gad, Glutamate Dehydrogenase. *P < 0.05, **P < 0.01, ***P < 0.001. (For interpretation of the references to color in this figure legend, the reader is referred to the web version of this article.)

As shown in Fig. 6M, after a 3-month intervention, the cortical mRNA expressions of Glul, Gls1 and Gls2 in db/db mice were reduced compared to the C57 mice, while the Gad1 mRNA expression was opposite ($P < 0.05$). The levels of Glul and Gls2 mRNA in the db LD group were elevated compared to the db RC group, while Gad1 mRNA expression was reduced ($P < 0.05$). Additionally, the db HD group exhibited increased Glul, Gls1, and Gls2 mRNA expression, but lower Gad1 and Gad2 mRNA level than the db RC group ($P < 0.05$).

After 6 months of intervention, the expressions of Glul, Gls1, Gad1 and Gad2 mRNA in the cerebral cortex of db/db mice were lower compared to those in the C57 group, but the Gls2 mRNA expression was opposite ($P < 0.05$). After a low-dose n-3 PUFA intervention, the cortical Gls2 mRNA expression was lower than that in db RC mice, while the expressions of Gad1 and Gad2 were higher than those in db RC mice ($P < 0.05$). After a high-dose n-3 PUFA dietary intervention, the expressions of Glul, Gls1 and Gad2

were higher than those of db RC mice, whereas the Gls2 was lower than that of db RC mice ($P < 0.05$, Fig. 6M).

Discussion

Insulin resistance, the core mechanism of T2DM, is implicated in cognitive decline and AD pathology in the elderly [3]. As a hallmark of metabolic syndrome, visceral obesity has been directly implicated in AD risk through systemic inflammation and insulin resistance, and cardiovascular metabolic factors like obesity prime the brain for neurodegeneration [25]. Against this background, our study explored how impaired glucose metabolism affects insulin signaling, and mitochondrial function in AD mice. We found that HFD induced insulin resistance and spontaneous diabetes worsen the AD-like pathology of mice. db/db mice exhibited disrupted brain insulin signaling, mitochondrial dysfunction and abnormal glutamine metabolism.

The typical pathological of AD are A β deposition, excessive phosphorylation of Tau protein, neuroinflammation, and neuronal loss [26]. First, regarding A β metabolism, animal experiments revealed that HFD-fed mice exhibit cognitive dysfunction due to increased brain A β content [26]. Al-Kuraishy et al. further emphasize the role of A β in disrupting organelle crosstalk, including mitochondria, which may explain the observed bioenergetic failure in HFD-fed APP/PS1 mice [27]. Correspondingly, HFD can enhance the APP cleavage and A β production, worsening AD pathology. However, results varied across genotypes: in APP/PS1 mice on HFD, APP and BACE1 proteins don't change significantly, perhaps due to the genotype. Lin et al. found no increased A β deposition in 5xFAD mice-fed with HFD [28]. Wakabayashi's research showed that HFD reduced A β clearance in A7 transgenic mice (overexpressing the human APP695 gene), while the levels of sAPP, sAPP α , sAPP β were not changed [29]. Second, for Tau phosphorylation, HFD didn't worsen central Tau protein in C57 or APP/PS1 mice, but increased Tau phosphorylation in APP/PS1 mice cortex, not in wide-type mice, suggesting that APP mutations enhanced Tau phosphorylation sensitivity in the brains of HFD-fed mice [30]. This indicates that AD-phenotype or genetic risk animals are more susceptible to develop AD-like brain pathological with HFD.

Regarding neuroinflammation, GFAP overexpression indicates astrocyte activation and marks brain inflammatory [30]. HFD enhanced GFAP expression in the cortex of both C57 and APP/PS1 mice, triggering neuroinflammation. Additionally, the cortical GFAP in mice from the HFD group exhibited an aggregated distribution, whereas it was diffusely distributed in db/db mice, and the central inflammatory area was more extensive compared to HFD mice. The mechanism involves periphery inflammatory cytokines crossing the blood-brain barrier (BBB), entering the central nervous system (CNS), activating microglia and astrocytes [31], and inducing the release of various pro-inflammatory factors, forming a feedback regulatory mechanism that worsens neuroinflammation [32]. Consistently, our data suggested that neuroinflammation is a shared cause of neurodegeneration in both T2DM and AD.

On signaling pathways, glycogen synthase kinase-3 (GSK3) is the primary kinase for excessive Tau phosphorylation. Phosphorylation at Tyr216 site is the activated form of GSK3, while phosphorylation at Ser9 and Ser389 sites are inactive forms [33]. Our results indicated that AD pathological status and HFD intervention did not affect the expression and activation of IR, IRS1, and GSK3 β proteins in the brains of APP/PS1 mice. This finding contrasts with previous reports that GSK3 β overactivation is closely associated with tau phosphorylation and A β deposition, and its abnormalities are commonly observed in AD animal models and human brain tissues [34]. The lack of changes in GSK3 β in this study may be attributed to factors such as the analysis of specific brain tissue regions (cortical homogenates potentially masking regional differences), mouse age (no GSK3 β abnormalities were detected at the time point of measurement), or model characteristics (genetic background, duration of HFD intervention, etc.). This result suggests that the regulatory mechanisms of AD-related signaling pathways are complex. Further exploration of the role of GSK3 β in AD, incorporating brain region-specific analysis and dynamic time-point detection, is necessary to better explain the discrepancies in conclusions across studies.

Cortical insulin resistance occurred in 7-months-old db/db mice, while mitochondria structural damage was evident in 4-month-old db/db mice. This suggests that cortical mitochondrial damage precedes cortical insulin resistance. Mitochondrial transport and dynamics are mutually regulated to maintain mitochondrial homeostasis [35]. In the cortex of AD patients, mitochondrial fission protein levels increase, while fusion protein expression levels decrease [36]. This increased mitochondrial fis-

sion damages the integrity of mitochondrial cristae and the localization of oxidative phosphorylation complexes in the inner membrane of mitochondria, adversely affecting energy generation and leading to synaptic dysfunction [37]. Similar alterations in mitochondrial dynamics were also observed in the brains of T2DM models induced by HFD. The expression and phosphorylation levels of Drp1 were upregulated in the hippocampus of T2DM mice compared to control mice. However, the expression levels of mitochondrial fusion proteins Mfn1/2 (Mfn1/2) and optic atrophy factor 1 (Opa1) showed no statistically significant alterations between the two groups [38]. Our study found the mitochondrial dynamics disorder in the cortex of db/db mice. The decreased L-Opa1/S-Opa1 ratio in the cortex of the APP HFD group indicates impaired mitochondrial fusion, a critical factor of mitochondrial network integrity. This imbalance likely disrupts the homeostasis of mitochondrial dynamics, resulting in fragmented mitochondria. Additionally, the opposite trend in hippocampal Fis1 expression (increased fission protein) suggests a regional specificity in mitochondrial stress responses, possibly driven by the hippocampus's heightened susceptibility to A β -induced pathology and metabolic stress from HFD.

4-month-old db/db mice exhibited impaired spatial memory, and 7-month-old db/db mice showed more severe cognitive dysfunction. db/db mice also exhibited AD-like pathological, GSK3 β expression reduced, while p-Ser9 GSK3 β and p-Ser396 Tau were increased. This may be a compensatory or protective mechanism induced by p-Tau. In db/db mice, the p-tau/tau ratio in the hippocampus and cortex was significantly elevated, and this increase was positively correlated with impaired learning and memory abilities [39]. HFD-induced metabolic abnormalities accelerate the deposition of hyperphosphorylated tau aggregates in tau transgenic mice, concomitant with neurodegeneration and behavioral deficits [40]. Notably, these pathological findings align with clinical observations: cerebrospinal fluid (CSF) levels of AD-associated phosphorylated tau markers are elevated in diabetic patients, and brain tau deposition correlates positively with hemoglobin A1c (HbA1c) levels [41].

Mitochondrial fragmentation in vulnerable brain regions such as the hippocampus, may exacerbate oxidative stress, disrupt synaptic mitochondrial distribution, and impair synaptic plasticity—critical mechanisms linked to cognitive decline in AD. These findings are consistent with previous studies indicating that Opa1 dysfunction contributes to neuronal dysfunction in neurodegenerative models [42,43]. This underscores the importance of considering disruptions in mitochondrial dynamics within the broader context of energy metabolism deficits and neuronal damage associated with AD.

Abnormal cellular energy production, caused by impaired mitochondrial function in the TCA cycle, has been identified as a common mechanism linking AD and T2DM [44]. Disruptions in the TCA cycle can directly affect central glucose metabolism, thereby promoting the development of diabetes-related cognitive dysfunction [45]. The number of TCA cycles in hippocampus, cortex, and striatum of diabetes mice with cognitive dysfunction is reduced [46]. Several TCA cycle intermediates, such as succinic acid and citric acid, also exhibit dysfunction in the hippocampus of these mice [14]. Citrate synthase (CS), isocitrate dehydrogenase (IDH), and alpha-ketoglutarate dehydrogenase complex (OGDH) are rate-limiting enzymes of the TCA cycle. Moreover, IDH2 deficiency leads to mitochondrial dysfunction under HFD-induced metabolic stress, characterized by decreased levels of NAD⁺ and NADH [47]. In this study, the diabetes status may interfere with IDH2 gene expression, potentially hindering the production of IDH enzyme. However, n-3 PUFA effectively alleviated the down-regulation of IDH2 gene expression caused by abnormal glucose metabolism, thereby improving mitochondrial function.

During energy generation, mitochondria oxidize NADH to NAD⁺, and the NAD⁺/NADH ratio decreases when mitochondria experience functional impairment [48]. Excessive electrons provided by NADH to mitochondria, can lead to functional damage in mitochondrial complex I and creating a vicious cycle when the redox state of NAD⁺/NADH is imbalanced [49]. This study found that intervention with n-3 PUFA increased the content of cortical NAD⁺ and the NAD⁺/NADH ratio, thereby improved mitochondrial function.

The effect of n-3 PUFA on glucose metabolism or insulin sensitivity in T2DM patients remains controversial [50–54]. n-3 PUFA intervention for 3 or 6 months did not improve the abnormal increase in FBG of db/db mice. One possible reason may be the different sources of n-3 PUFA. Plant-derived α -Linolenic acid improved blood glucose, animal-derived Eicosapentaenoic Acid and DHA influenced blood lipids [18]. In db/db mice, n-3 PUFA reduced liver weight and lipid deposition dose-dependently. Besides, triglycerides form n-3 PUFA used in our study may weaken the absorption, since the phosphatidylcholine form is preferred [18]. The study does not directly address GLP-1 agonists; however, it has demonstrated that sitagliptin enhances insulin signaling in non-diabetic contexts, suggesting shared pathways in metabolic regulation [55].

Studies indicated that T2DM patients exhibit slower information processing speeds, and DTI scans revealed changes in white matter, suggesting cognitive dysfunction associated with impaired brain fiber bundles [56]. However, our study found no nerve fiber bundles structure changes. Moreover, the number of neurons decreased in the db/db mice, but 6-months n-3 PUFA dietary intervention prevented the disorder. n-3 PUFA deficiency shortened hippocampal neurons axons, while supplementation with n-3 PUFA restored the length of axons [57]. n-3 PUFA exerts anti-apoptotic effects by increasing the content of phosphatidylserine on the neuronal cell membrane [58]. The observed benefits of n-3 PUFA also align with emerging interest in nutraceuticals for early AD prevention, particularly in populations with metabolic comorbidities [59–62]. We speculate that cognitive dysfunction of db/db mice was not caused by brain nerve fibers structure changes, but neurons loss or apoptosis, and n-3 PUFA may alleviate neuronal loss, promoting neurogenesis and recovery of diabetes-related cognitive dysfunction.

Brain insulin resistance arises from impaired brain cells response to insulin or reduced insulin transport to the brain [63]. The brain, an insulin-sensitive organ, allows peripheral insulin cross the BBB, concentrating in the hypothalamus [64]. In the CNS, insulin regulates synaptic function, neuronal survival, and glucose metabolism, vital for feeding, energy metabolism, and cognitive functions [65]. Under physiological conditions, insulin binds to the Insulin Receptor (IR), activating the IRSs/PI3K/AKT involved in brain glucose metabolism, A β clearance, and GSK3 activation [66]. High neuroinflammation disrupts hippocampal insulin signaling by increasing IRS1 serine phosphorylation [67]. The study revealed the increased phosphorylation of IR, AKT, and GSK3 β proteins in the cortex of db/db mice. HFD and db/db mice exhibited central insulin resistance within the cortical region, accompanied by a marked increase in p-IRS1 at the Ser307 residue. n-3 PUFA intervention did not alter cortical insulin levels in db/db mice, but reversed the abnormal increase in *insulin 1* mRNA expression, and the insulin level in the cortex of mice also increases with ageing of mice. These findings suggest that HFD may promote central insulin resistance in C57 mice by inducing central inflammation, whereas in db/db mice, it could result from both inflammation and disrupted insulin signaling. The cortex of db/db mice displays aberrant activation of the insulin signaling pathway in the early stage of T2DM. Under the sustained effect of the disease phenotype, the sensitivity of cortical neurons to insulin decreased, and the insulin signaling pathway became dysfunctional. However, a

high-dose n-3 PUFA intervention improved the dysfunction of the cortical insulin signaling pathway in db/db mice.

This study has several limitations. Firstly, small sample sizes pose a risk of unreliable results due to compromised reproducibility from individual and environmental variability, biased effect estimates, and missed rare subgroup differences. Solutions for our future research include the promotion of in vitro models as complementary tools and establishment of cross-institutional data platforms for meta-analytic integration, thereby enhancing reliability. Secondly, the pathological features of db/db mice in the T2DM model are attributed to the knockout of the leptin receptor. However, the occurrence of T2DM in humans is multifactorial. Consequently, the changes observed in db/db mice cannot fully represent the true biological characteristics of T2DM patients, and the extrapolation of these results has certain limitations. Thirdly, the dosage and duration of n-3 PUFA intervention were determined based on published literature and our previous findings [68]. Future research should investigate whether varying intervention conditions yield different outcomes, conduct a comprehensive exploration of protein-coding genes from multidimensional perspectives, validate findings in different animal models, and explore possible mechanisms through in vitro experiments, with the aim of translating optimal results and providing evidence for clinical applications. Given that diabetic patients typically take medications, future studies should also explore the interactions between n-3 PUFA interventions and drugs using through randomized controlled trials (RCTs) or other population-based studies.

Conclusion

Our research revealed the following key points: (1) Compared with insulin-resistant mice induced by HFD, the brain cortex of spontaneous diabetes model db/db mice exhibited pronounced insulin resistance and mitochondrial dysfunction. (2) In the context of AD combined with insulin resistance, the disorder of brain mitochondrial energy metabolism and glutamate-glutamine circulation in mice may constitute the pathological basis for diabetes-related cognitive dysfunction. (3) Increasing dietary intake of n-3 PUFA can ameliorate insulin resistance in db/db mice, prevent neuronal loss, and alleviate abnormalities in brain mitochondrial structure and function. (4) n-3 PUFA can facilitate the recovery of cognitive function in db/db mice by regulating cortical mitochondrial energy metabolism and enhancing the glutamate-glutamine cycle.

Ethical Statement

The study was conducted in accordance with the Regulations for Administration of Affairs Concerning Experimental Animals guidelines and approved protocols of Capital Medical University (AEEI-2019-008).

Funding Sources

This study was supported by the grants from the National Natural Science Foundation of China (No. 82173508, No. 82304132), Nutrilite Plant Functional Components and Health Research Fund of Chinese Nutrition Society (No. CNS-NCL2024-04) and Science and technology project of Suzhou Health Commission (No. MSXM2024079).

CRedit authorship contribution statement

Yu Liu: Conceptualization, Methodology, Data curation, Software, Writing – original draft. **Xiaojun Ma:** Conceptualization,

Methodology, Data curation, Software, Writing – original draft. **Jingjing Xu:** Investigation. **Xixiang Wang:** Investigation. **Lu Liu:** Investigation. **Xiuwen Ren:** Investigation. **Chi Zhang:** Writing – review & editing. **Shaobo Zhou:** Writing – review & editing. **Ying Wang:** Writing – review & editing, Funding acquisition. **Xinjing Guo:** Supervision, Writing – review & editing, Funding acquisition. **Linhong Yuan:** Supervision, Writing – review & editing, Funding acquisition.

Declaration of competing interest

The authors declare that they have no known competing financial interests or personal relationships that could have appeared to influence the work reported in this paper.

Acknowledgement

The authors thank the support provided by the Core Facility Center of Capital Medical University.

Appendix A. Supplementary data

Supplementary data to this article can be found online at <https://doi.org/10.1016/j.jare.2025.06.044>.

References

- Biessels GJ, Whitmer RA. Cognitive dysfunction in diabetes: how to implement emerging guidelines. *Diabetologia* 2020;63(1):3–9. doi: <https://doi.org/10.1007/s00125-019-04977-9>.
- Livingston G, Huntley J, Sommerlad A, et al. Dementia prevention, intervention, and care: 2020 report of the Lancet Commission. *Lancet* 2020;396(10248):413–46. doi: [https://doi.org/10.1016/S0140-6736\(20\)30367-6](https://doi.org/10.1016/S0140-6736(20)30367-6).
- Gadhav K, Kumar D, Uversky VN, Giri R. A multitude of signaling pathways associated with Alzheimer's disease and their roles in AD pathogenesis and therapy. *Med Res Rev* 2021;41(5):2689–745. doi: <https://doi.org/10.1002/med.21719>.
- Heydarpour F, Sajadimajid S, Mirzarazi E, et al. Involvement of TGF- β and autophagy pathways in pathogenesis of diabetes: a comprehensive review on biological and pharmacological insights. *Front Pharmacol* 2020;11:498758. doi: <https://doi.org/10.3389/fphar.2020.498758>.
- Norins LC. Repurposing licensed drugs for use against Alzheimer's disease. *J Alzheimers Dis* 2021;81(3):921–32. doi: <https://doi.org/10.3233/JAD-210080>.
- Liu Q, Wang Z, Cao J, Dong Y, Chen Y. The role of insulin signaling in hippocampal-related diseases: a focus on Alzheimer's disease. *Int J Mol Sci* 2022;23(22):14417. doi: <https://doi.org/10.3390/ijms232214417>.
- Al Hussein Al Awamlh S, Wareham LK, Risner ML, Calkins DJ. Insulin signaling as a therapeutic target in glaucomatous neurodegeneration. *Int J Mol Sci* 2021;22(9):4672. doi: <https://doi.org/10.3390/ijms22094672>.
- Girault FM, Sonnay S, Gruetter R, Duarte JMN. Alterations of brain energy metabolism in type 2 diabetic Goto-Kakizaki Rats measured In Vivo by ¹³C magnetic resonance spectroscopy. *Neurotox Res* 2019;36(2):268–78. doi: <https://doi.org/10.1007/s12640-017-9821-y>.
- Duarte JMN, Skoug C, Silva HB, Carvalho RA, Gruetter R, Cunha RA. Impact of caffeine consumption on type 2 diabetes-induced spatial memory impairment and neurochemical alterations in the hippocampus. *Front Neurosci* 2019;12:1015. doi: <https://doi.org/10.3389/fnins.2018.01015>.
- Li S, Sheng ZH. Energy matters: presynaptic metabolism and the maintenance of synaptic transmission. *Nat Rev Neurosci* 2022;23(1):4–22. doi: <https://doi.org/10.1038/s41583-021-00535-8>.
- Cerasuolo M, Papa M, Colangelo AM, Rizzo MR. Alzheimer's disease from the amyloidogenic theory to the puzzling crossroads between vascular, metabolic and energetic maladaptive plasticity. *Biomedicines* 2023;11(3):861. doi: <https://doi.org/10.3390/biomedicines11030861>.
- Cerasuolo M, Di Meo I, Auriemma MC, et al. Iron and ferroptosis more than a suspect: beyond the most common mechanisms of neurodegeneration for new therapeutic approaches to cognitive decline and dementia. *Int J Mol Sci* 2023;24(11):9637. doi: <https://doi.org/10.3390/ijms24119637>.
- Hirase S, Tezuka A, Nagano AJ, et al. Integrative genomic phylogeography reveals signs of mitonuclear incompatibility in a natural hybrid goby population. *Evolution* 2021;75(1):176–94. doi: <https://doi.org/10.1111/evo.14120>.
- To M, Sugimoto M, Saruta J, et al. Cognitive dysfunction in a mouse model of cerebral ischemia influences salivary metabolomics. *J Clin Med* 2021;10(8):1698. doi: <https://doi.org/10.3390/jcm10081698>.
- Yin F. Lipid metabolism and Alzheimer's disease: clinical evidence, mechanistic link and therapeutic promise. *FEBS J* 2023;290(6):1420–53. doi: <https://doi.org/10.1111/febs.16344>.
- Woodfield A, Gonzales T, Helmerhorst E, et al. Current insights on the use of insulin and the potential use of insulin mimetics in targeting insulin signalling in Alzheimer's disease. *Int J Mol Sci* 2022;23(24):15811. doi: <https://doi.org/10.3390/ijms232415811>.
- Wang L, Huang X, Sun M, et al. New light on ω -3 polyunsaturated fatty acids and diabetes debate: a population pharmacokinetic-pharmacodynamic modelling and intake threshold study. *Nutr Diabetes* 2024;14:8. doi: <https://doi.org/10.1038/s41387-024-00262-w>.
- Khan I, Hussain M, Jiang B, et al. Omega-3 long-chain polyunsaturated fatty acids: metabolism and health implications. *Prog Lipid Res* 2023;92:101255. doi: <https://doi.org/10.1016/j.plipres.2023.101255>.
- von Schacky C. Importance of EPA and DHA blood levels in brain structure and function. *Nutrients* 2021;13(4):1074. doi: <https://doi.org/10.3390/nu13041074>.
- Othman MZ, Hassan Z, Che Has AT. Morris water maze: a versatile and pertinent tool for assessing spatial learning and memory. *Exp Anim* 2022;71(3):264–80. doi: <https://doi.org/10.1538/expanim.21-0120>.
- Hussaini HM, Seo B, Rich AM. Immunohistochemistry and Immunofluorescence. *Methods Mol Biol* 2023;2588:439–50. doi: https://doi.org/10.1007/978-1-0716-2780-8_26.
- Yi KS, Choi CH, Jung C, et al. Which pathologic staining method can visualize the hyperacute infarction lesion identified by diffusion MRI?: A comparative experimental study. *J Neurosci Methods* 2020;344:108838. doi: <https://doi.org/10.1016/j.jneumeth.2020.108838>.
- Kim SH, Shin HL, Son TH, et al. Quercus glauca acorn seed coat extract promotes wound re-epithelialization by facilitating fibroblast migration and inhibiting dermal inflammation. *Biology (Basel)* 2024;13(10):775. doi: <https://doi.org/10.3390/biology13100775>.
- Ruiz-Rizzo AL, Finke K, Archila-Meléndez ME. Diffusion tensor imaging in Alzheimer's studies. *Methods Mol Biol* 2024;2785:105–13. doi: https://doi.org/10.1007/978-1-0716-3774-6_8.
- Al-Kuraishy HM, Al-Gareeb AI, Alsayegh AA, Hakami ZH, Khamjan NA, Saad HM, et al. A potential link between visceral obesity and risk of Alzheimer's disease. *Neurochem Res* 2023;48(3):745–66.
- Espinosa-Jiménez T, Cano A, Sánchez-López E, et al. A novel rhein-huprine hybrid ameliorates disease-modifying properties in preclinical mice model of Alzheimer's disease exacerbated with high fat diet. *Cell Biosci* 2023;13(1):52. doi: <https://doi.org/10.1186/s13578-023-01000-y>.
- Al-Kuraishy HM, Sulaiman GM, Mohammed HA, Mohammed SG, Al-Gareeb AI, Albuhadily AK, et al. Amyloid- β and heart failure in Alzheimer's disease: the new vistas. *Front Med* 2025;4(12):1494101.
- Fu Y, Gu Z, Cao H, et al. The role of the gut microbiota in neurodegenerative diseases targeting metabolism. *Front Neurosci* 2024;18:1432659. doi: <https://doi.org/10.3389/fnins.2024.1432659>.
- Lv YQ, Yuan L, Sun Y, et al. Long-term hyperglycemia aggravates α -synuclein aggregation and dopaminergic neuronal loss in a Parkinson's disease mouse model. *Transl Neurodegener* 2022;11(1):14. doi: <https://doi.org/10.1186/s40035-022-00288-z>.
- Ettheto M, Sánchez-Lopez E, Cano A, et al. Dexibuprofen ameliorates peripheral and central risk factors associated with Alzheimer's disease in metabolically stressed APP^{swe}/PS1^{dE9} mice. *Cell Biosci* 2021;11(1):141. doi: <https://doi.org/10.1186/s13578-021-00646-w>.
- Verkhatsky A, Butt A, Li B, et al. Astrocytes in human central nervous system diseases: a frontier for new therapies. *Signal Transduct Target Ther* 2023;8(1):396. doi: <https://doi.org/10.1038/s41392-023-01628-9>.
- Silveira ASA, Alves ACDA, Gimenes GM, et al. Evidence for a Pro-inflammatory state of macrophages from non-obese type-2 diabetic Goto-Kakizaki rats. *Int J Mol Sci* 2024;25(19):10240. doi: <https://doi.org/10.3390/ijms251910240>.
- Cap KC, Jung YJ, Choi BY, et al. Distinct dual roles of p-Tyr42 RhoA GTPase in tau phosphorylation and ATP citrate lyase activation upon different A β concentrations. *Redox Biol* 2020;32:101446. doi: <https://doi.org/10.1016/j.redox.2020.101446>.
- Shri SR, Manandhar S, Nayak Y, Pai KSR. Role of GSK-3 β inhibitors: new promises and opportunities for Alzheimer's disease. *Adv Pharm Bull* 2023;13(4):688–700. doi: <https://doi.org/10.34172/apb.2023.071>.
- Luo JS, Ning JQ, Chen ZY, et al. The role of mitochondrial quality control in cognitive dysfunction in diabetes. *Neurochem Res* 2022;47(8):2158–72. doi: <https://doi.org/10.1007/s11064-022-03631-y>.
- Ali J, Choe K, Park JS, et al. The interplay of protein aggregation, genetics, and oxidative stress in Alzheimer's disease: role for natural antioxidants and immunotherapeutics. *Antioxidants (Basel)* 2024;13(7):862. doi: <https://doi.org/10.3390/antiox13070862>.
- Johri A. Disentangling mitochondria in Alzheimer's disease. *Int J Mol Sci* 2021;22(21):11520. doi: <https://doi.org/10.3390/ijms222111520>.
- Cervantes-Silva MP, Carroll RG, Wilk MM, et al. The circadian clock influences T cell responses to vaccination by regulating dendritic cell antigen processing. *Nat Commun* 2022;13(1):7217. doi: <https://doi.org/10.1038/s41467-022-34897-z>.
- Morys F, Potvin O, Zeighami Y, et al. Obesity-associated neurodegeneration pattern mimics Alzheimer's disease in an observational cohort study. *J Alzheimers Dis* 2023;91(3):1059–71. doi: <https://doi.org/10.3233/JAD-220535>.
- Liang Z, Gong X, Ye R, et al. Long-term high-fat diet consumption induces cognitive decline accompanied by tau hyper-phosphorylation and microglial activation in aging. *Nutrients* 2023;15(1):250. doi: <https://doi.org/10.3390/nu15010250>.

- [41] Michailidis M, Moraitou D, Tata DA, Kalinderi K, Papamiou T, Papaliagkas V. Alzheimer's disease as type 3 diabetes: common pathophysiological mechanisms between Alzheimer's disease and type 2 diabetes. *Int J Mol Sci* 2022;23(5):2687. doi: <https://doi.org/10.3390/ijms23052687>.
- [42] Grel H, Woznica D, Ratajczak K, et al. Mitochondrial dynamics in neurodegenerative diseases: unraveling the role of fusion and fission processes. *Int J Mol Sci* 2023;24(17):13033. doi: <https://doi.org/10.3390/ijms241713033>.
- [43] Tábara LC, Segawa M, Prudent J. Molecular mechanisms of mitochondrial dynamics. *Nat Rev Mol Cell Biol* 2025;26(2):123–46. doi: <https://doi.org/10.1038/s41580-024-00785-1>.
- [44] Butterfield DA, Boyd-Kimball D, Reed TT. Cellular stress response (hormesis) in response to bioactive nutraceuticals with relevance to Alzheimer disease. *Antioxid Redox Signal* 2023;38(7–9):643–69. doi: <https://doi.org/10.1089/ars.2022.0214>.
- [45] Zhang S, Zhang Y, Wen Z, et al. Cognitive dysfunction in diabetes: abnormal glucose metabolic regulation in the brain. *Front Endocrinol (Lausanne)* 2023;14:1192602. doi: <https://doi.org/10.3389/fendo.2023.1192602>.
- [46] Xu P, Ning J, Jiang Q, et al. Region-specific metabolic characterization of the type 1 diabetic brain in mice with and without cognitive impairment. *Neurochem Int* 2021;143:104941. doi: <https://doi.org/10.1016/j.neuint.2020.104941>.
- [47] Lee JH, Go Y, Kim DY, et al. Isocitrate dehydrogenase 2 protects mice from high-fat diet-induced metabolic stress by limiting oxidative damage to the mitochondria from brown adipose tissue. *Exp Mol Med* 2020;52(2):238–52. doi: <https://doi.org/10.1038/s12276-020-0379-z>.
- [48] Jiang X, Baig AH, Palazzo G, et al. P53-dependent hypusination of eIF5A affects mitochondrial translation and senescence immune surveillance. *Nat Commun* 2024;15(1):7458. doi: <https://doi.org/10.1038/s41467-024-51901-w>.
- [49] Denmark D, Ruhoy I, Wittmann B, Ashki H, Koran LM. Altered plasma mitochondrial metabolites in persistently symptomatic individuals after a GBCA-assisted MRI. *Toxics* 2022;10(2):56. doi: <https://doi.org/10.3390/toxics10020056>.
- [50] Neuenschwander M, Barbaresko J, Pischke CR, et al. Intake of dietary fats and fatty acids and the incidence of type 2 diabetes: a systematic review and dose-response meta-analysis of prospective observational studies. *PLoS Med* 2020;17(12):e1003347. doi: <https://doi.org/10.1371/journal.pmed.1003347>.
- [51] Yang W, Jiang W, Guo S. Regulation of macronutrients in insulin resistance and glucose homeostasis during Type 2 Diabetes Mellitus. *Nutrients* 2023;15(21):4671. doi: <https://doi.org/10.3390/nu15214671>.
- [52] Al-Shaer AE, Buddenbaum N, Shaikh SR. Polyunsaturated fatty acids, specialized pro-resolving mediators, and targeting inflammation resolution in the age of precision nutrition. *Biochim Biophys Acta Mol Cell Biol Lipids* 2021;1866(7):158936. doi: <https://doi.org/10.1016/j.bbalip.2021.158936>.
- [53] Grytten E, Laupsa-Borge J, Cetin K, et al. Inflammatory markers after supplementation with marine n-3 or plant n-6 PUFAs: a randomized double-blind crossover study. *J Lipid Res* 2025;66(4):100770. doi: <https://doi.org/10.1016/j.jlr.2025.100770>.
- [54] Saros L, Vahlberg T, Koivuniemi E, et al. Fish oil and/or probiotics intervention in overweight/obese pregnant women and overweight risk in 24-month-old children. *J Pediatr Gastroenterol Nutr* 2023;76(2):218–26. doi: <https://doi.org/10.1097/MPG.0000000000003659>.
- [55] Al-Kuraishy HM, Al-Gareeb AI, Qusty N, Alexiou A, Batiha GE. Impact of sitagliptin on non-diabetic Covid-19 patients. *Curr Mol Pharmacol* 2022;15(4):683–92.
- [56] Li Y, Liu Y, Liu S, et al. Diabetic vascular diseases: molecular mechanisms and therapeutic strategies. *Signal Transduct Target Ther* 2023;8(1):152. doi: <https://doi.org/10.1038/s41392-023-01400-z>.
- [57] Petermann AB, Reyna-Jeldes M, Ortega L, Coddou C, Yévenes GE. Roles of the unsaturated fatty acid docosahexaenoic acid in the central nervous system: molecular and cellular insights. *Int J Mol Sci* 2022;23(10):5390. doi: <https://doi.org/10.3390/ijms23105390>.
- [58] Gao J, Cheng B, Sun Y, Zhao Y, Zhao G. Effects of dietary inclusion with rapeseed cake containing high glucosinolates on nitrogen metabolism and urine nitrous oxide emissions in steers. *Anim Nutr* 2022;8(1):204–15. doi: <https://doi.org/10.1016/j.aninu.2021.05.006>.
- [59] Al-Kuraishy HM, Al-Gareeb AI, Alsayegh AA, Abusudah WF, Almohmadi NH, Eldahshan OA, et al. Insights on benzodiazepines' potential in Alzheimer's disease. *Life Sci* 2023;1(320):121532.
- [60] Al-Kuraishy HM, Sulaiman GM, Mohammed HA, Al-Gareeb AI, Albuhadily AK, Mohammed SG. Role of RhoA-ROCK signaling inhibitor fasudil in Alzheimer disease. *Behav Brain Res* 2025;3:115524.
- [61] Batiha GE, Wasef L, Teibo JO, Shaheen HM, Zakariya AM, Akinfe OA, et al. *Commiphora myrrh*: a phytochemical and pharmacological update. *Naunyn Schmiedeberg Arch Pharmacol* 2023;396(3):405–20.
- [62] Al-Kuraishy HM, Al-Gareeb AI, Zekry SH, Alruwaili M, Alexiou A, Papadakis M, et al. The possible role of cerebrolysin in the management of vascular dementia: leveraging concepts. *Neuroscience* 2025.
- [63] Rhea EM, Leclerc M, Yassine HN, et al. State of the science on brain insulin resistance and cognitive decline due to Alzheimer's disease. *Aging Dis* 2024;15(4):1688–725. doi: <https://doi.org/10.14336/AD.2023.0814>.
- [64] Lin KJ, Wang TJ, Chen SD, et al. Two birds one stone: the neuroprotective effect of antidiabetic agents on Parkinson disease-focus on sodium-glucose cotransporter 2 (SGLT2) inhibitors. *Antioxidants (Basel)* 2021;10(12):1935. doi: <https://doi.org/10.3390/antiox10121935>.
- [65] Picone P, Sanfilippo T, Vasto S, et al. From small peptides to large proteins against Alzheimer's disease. *Biomolecules* 2022;12(10):1344. doi: <https://doi.org/10.3390/biom12101344>.
- [66] Agrawal R, Reno CM, Sharma S, Christensen C, Huang Y, Fisher SJ. Insulin action in the brain regulates both central and peripheral functions. *Am J Phys Endocrinol Metab* 2021;321(1):E156–63. doi: <https://doi.org/10.1152/ajpendo.00642.2020>.
- [67] Wittwer J, Bradley D. Clusterin and its role in insulin resistance and the cardiometabolic syndrome. *Front Immunol* 2021;12:612496. doi: <https://doi.org/10.3389/fimmu.2021.612496>.
- [68] Ma X, Guo Y, Xu J, et al. Effects of distinct n-6 to n-3 polyunsaturated fatty acid ratios on insulin resistant and AD-like phenotypes in high-fat diets-fed APP/PS1 mice. *Food Res Int* 2022;162(Pt B):112207. doi: <https://doi.org/10.1016/j.foodres.2022.112207>.